ADVANCED MATERIALS

Thermomechanical Lithography: Pattern Replication Using a Temperature Gradient Driven Instability**

By *Erik Schäffer*, *Stephan Harkema*, *Monique Roerdink*, *Ralf Blossey*, and *Ullrich Steiner**

The rapid pace of advancements in the semiconductor industry requires a continual decrease in the size of smallest features on integrated circuits.[1] For the wavelengths of light currently used, the smallest feasible structure sizes are approximately 100 nm, with the diffraction limit as a fundamental boundary. The extension of photolithography to even shorter wavelengths is a considerable technological challenge, since neither appropriate light sources (lasers) nor suitable optical elements are currently available. Electron- and ion-projection, proximity X-ray, and extreme-UV lithography attempt to extend optical projection techniques to smaller wavelengths. While the semiconductor industry is pursuing this approach, various techniques that are not based on projection have emerged. Small surface patterns can be written either by an electron or ion beam or by a large number of methods that employ a tip of a scanning probe microscope (e.g., near-field optical lithography or dip-pen lithography[2]). The main disadvantage of these "serial" techniques is, however, a very low throughput rate.

Alternative "parallel" methods involve pattern transfer by direct contact with a suitable structured master. This approach includes most notably microcontact printing and derived molding and casting techniques.[3] More recently, structure sizes of ~10 nm were achieved by nano-imprinting, hot embossing, and injection molding lithography.[4–6]

A somewhat less established approach makes use of surface instabilities in thin polymer films. While this principle was demonstrated by us for instabilities connected to a demixing process,[7] or triggered by electric fields,[8] it can be extended to nearly any interaction that causes a liquid surface to become unstable. The application and extension of this approach requires an understanding of hydrodynamic surface instabilities that lead to the break-up of thin liquid films. While such studies go back more than one century,[9,10] most recent work has focused on the dewetting of polymer films caused by van der Waals forces.[11–13] This was later extended to instabilities caused by elastic stresses[14] and electrostatic interactions.[8,15–17] Very recently, we have reported the break-up of thin films caused by temperature gradients[18,19] and by the confinement of thermal modes in a thin film.[20]

While conceptually diverse, these examples are governed by the same hydrodynamic mechanisms. Therefore, they all yield structures with similar morphologies. In our previous work, typical periodicities are on the order of several micrometers,[7,8,17–20] but length scales down to 100 nm have also been reported.[8] While a homogeneous force field acting at the surface of a planar film leads to patterns that are characterized by a single length scale, the imposition of a laterally varying force field can be used to direct the intrinsic instability to replicate a master pattern.[7,8]

Here, we demonstrate the combination of two of the principles described above: the destabilization of a thin polymer film that is exposed to a high-temperature gradient and pattern replication by laterally modulating a destabilizing force.

Our experimental system consisted of the two-plate assembly shown schematically in Figure 1. A polymer–air double

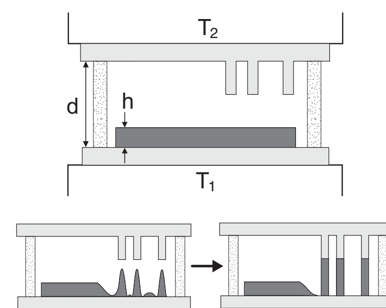

Fig. 1. Schematic representation of the experimental setup. A liquid polymer film (dark gray) of thickness h is sandwiched between two silicon substrates (light gray), one of which is topographically structured. The distance d between the substrates is controlled by silicon dioxide spacers (dotted). One substrate is heated to a temperature T_1 and the other cooled relative to it, to a temperature T_2. The temperature difference $\Delta T = T_1 - T_2$ results in a gradient normal to the film surface on the order of $\Delta T/d$, destabilizing the interface. With time, the initially flat film is drawn toward the downward protruding structures forming a positive replica of the master pattern.

layer was sandwiched between a planar and a topographically patterned plate, which were kept at different temperatures T_1 and T_2. This resulted in a redistribution of the polymer, as indicated in Figure 1. This effect is shown in Figure 2, where various hexagonal patterns (a–c) and cross-hatched lines (d) were reproduced. With a properly aligned setup, pattern replication extends defect free over the entire area covered by the master structures. This is illustrated in Figure 3, which shows low magnification micrographs taken of two locations on the same sample, which were 2.7 mm apart. The transferred pattern is a positive replica of the master relief. The structures protrude above the film's original thickness, thereby increasing the aspect ratio. This is analogous to electrostatic lithography,[8] but the opposite of the hot embossing technique where

[*] Prof. U. Steiner, Dr. E. Schäffer,[+] S. Harkema, M. Roerdink
Department of Polymer Chemistry and Materials Science Center
University of Groningen
NL-9747 AG Groningen (The Netherlands)
E-mail: u.steiner@chem.rug.nl
Dr. R. Blossey
Center for Bioinformatics, University of Saarland
D-66123 Saarbrücken (Germany)
[+] Present address: Max Planck Institute of Molecular Cell Biology and Genetics, D-01307 Dresden, Germany.

[**] We thank T. Thurn-Albrecht for stimulating discussions, W. Zulehner and Wacker-Chemie GmbH for the silicon wafers, and B. Maile and eXtreme Lithography for the master patterns. RB acknowledges support by the priority program of the DFG "Wetting and structure formation at surfaces". This work was partially funded by the Deutsche Forschungsgemeinschaft (DFG) through the Sonderforschungsbereich 513 and by the Dutch "Stichting voor Fundamenteel Onderzoek der Materie" (FOM).

 © 2003 WILEY-VCH Verlag GmbH & Co. KGaA, Weinheim 0935-9648/03/0603-0514 $ 17.50+.50/0 *Adv. Mater.* **2003**, *15*, No. 6, March 17

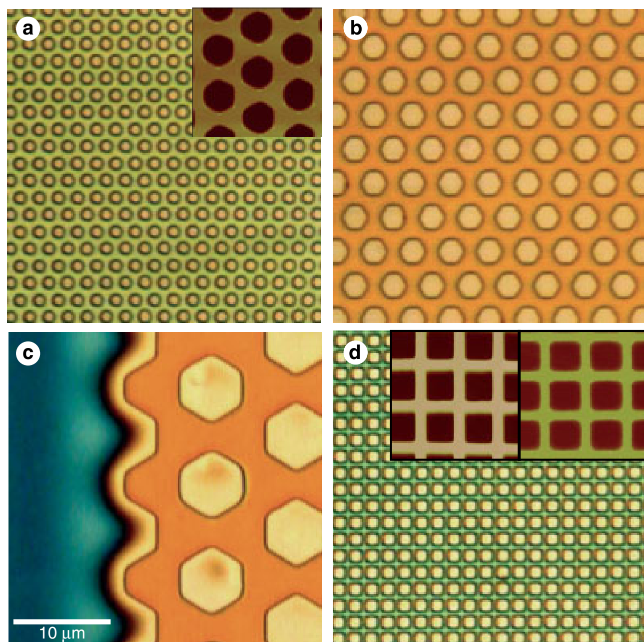

Fig. 2. Pattern replication in a polystyrene film using a structured top plate. The optical micrographs (a–c) were obtained on the same sample ($h = 106$ nm, $T_1 = 171$ °C, $T_2 = 133$ °C). The ordered hexagonal arrays had periodicities of 2 μm (a), 4 μm (b), and 10 μm (c). Due to a slight misalignment of the two plates with respect to each other, the plate spacing d varied from 160 nm in (a) to 220 nm in (c). In (d) an experiment ($h = 65$ nm, $d = 155$ nm) with an inverted temperature gradient is shown ($T_1 = 171$ °C, $T_2 = 189$ °C). The replicated cross-hatched pattern in (d) has a stripe width of 500 nm. The mechanism of a film instability in an inverted temperature gradient is described in the literature [19]. The colors stem from the constructive interference of the white microscope illumination and are an indication of local film thickness. The insets in (a) and (d) are higher magnification AFM images. The two insets in (d) compare the topographic structure of the master (left) and the replicated polymer pattern (right).

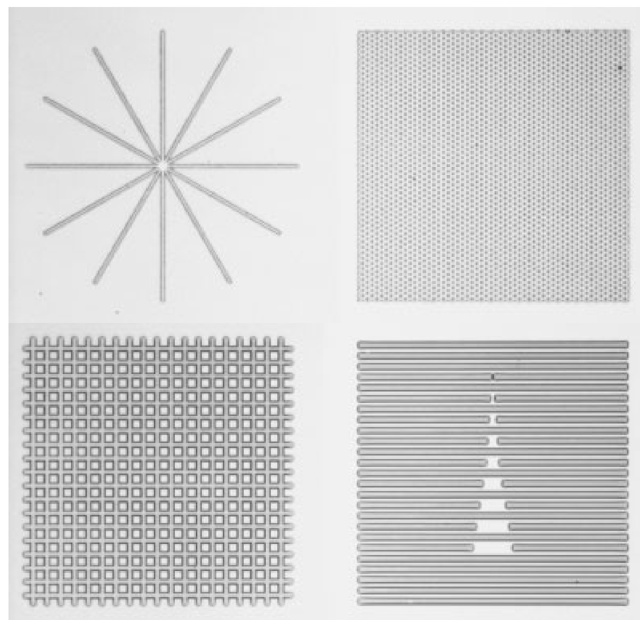

Fig. 3. Large area images of replicated patterns. To illustrate the fidelity of the replication process, optical micrographs of four 200 μm × 200 μm replicated areas are shown. The two top images were taken on the same sample as the two bottom images, at a lateral distance of 2.7 nm (comparable to the width of the structured area of the master). The sample was a 157 nm thick polystyrene film exposed to $\Delta T = 38$ K ($T_1 = 170$ °C, $T_2 = 132$ °C) for 20 h. The plate spacing d varied (over a lateral distance of 2.7 mm) from 170 nm (top left) to 220 nm (bottom right).

a template is pressed into a molten polymer film by high external forces resulting in a negative copy.[4]

To elucidate the origins of the pattern replication process, it is necessary to summarize the mechanisms that lead to the destabilization of a thin polymer film exposed to a high temperature gradient. A detailed description is given elsewhere.[18,19] In Figure 4 images are shown, in which the structured top plate in Figure 1 was replaced by a flat plate. Figure 4 shows an instability that was caused by an applied temperature gradient. Two different topographic morphologies were observed as a function of the ratio d/h, with columns for large values of d/h (Fig. 4a) and a striped morphology for small values of d/h (Fig. 4b).[19] Both the striped and columnar morphologies exhibit a single dominant lateral length scale λ that is characteristic of the experimental parameters of the sample.

Since convection effects are strongly suppressed in thin films of a highly viscous liquid, the pattern formation processes that are commonly caused by a temperature gradient (Rayleigh-Bénard or Bénard-Marangoni convection) can be ruled out. Instead, heat is transported across the polymer–air bilayer by diffusive mechanisms. In the polymer layer, molecular vibrations in the liquid transport the heat. This flux of thermal energy is given by Fourier's equation

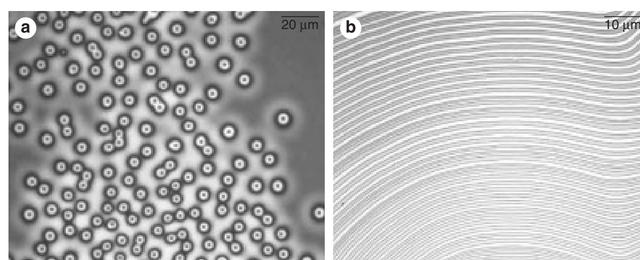

Fig. 4. Instabilities of polymer films exposed to laterally homogeneous temperature gradients. The optical micrographs show polystyrene films that were heated in a set-up similar to that shown in Figure 1, where the structured top plate was replaced by a flat plate. Columnar (a) and striped (b) patterns were observed, often on the same sample. Sample parameters were: a) $h = 106$ nm, $d = 448$ nm, $T_1 = 170$ °C, $T_2 = 124$ °C; b) $h = 100$ nm, $d = 202$ nm, $T_1 = 170$ °C, $T_2 = 133$ °C.

$$J_q = -\kappa \frac{\partial T}{\partial z} = \frac{\kappa_0 \kappa_p \Delta T}{\kappa_0 h + \kappa_p (d-h)} \tag{1}$$

where z is the normal coordinate and κ the thermal conductivity with the indices p and 0 referring to the polymer and air, respectively. The energy flux is associated with a momentum flux (J_p) in the direction of lower temperatures, $J_p = J_q/u$, with the velocity of sound in the polymer u. The reflection of the elastic waves (phonons) at the film surface due to the different acoustic impedances of the polymer and air exerts a pressure p which destabilizes the interface. This radiation pressure is given by

$$p = -2Q \frac{J_q}{u} \tag{2}$$

 © 2003 WILEY-VCH Verlag GmbH & Co. KGaA, Weinheim 0935-9648/03/0603-0515 $ 17.50+.50/0

The effective reflectivity or quality factor Q is a complex function of the frequency dependent reflection coefficients of all interfaces and the sound velocities of the three media (polymer, air, bounding plates). It has been calculated by integrating the heat flux and the Rayleigh pressure over the Debye density of states in the polymer layer, taking the different mechanisms of heat transport in the crystalline substrates, the glassy polymer melt, and the gas layer into account.[18,19] In the polymer film, the low- and high-frequency limits of the elastic wave spectrum have to be considered separately. Low-frequency modes have, compared to the film thickness, a long mean free path length in the polymer and propagate ballistically. They are nearly perfectly reflected at the polymer–air interface, exerting a large destabilizing pressure. On the other hand, high-frequency modes diffuse through the system and are well transmitted through the polymer–air interface. They ensure the overall heat conduction given by Fourier's equation. Additionally, they exert a small stabilizing pressure. The Q factor, which incorporates all these effects depends only on the materials properties of the setup and not on the geometry or temperature difference. For the silicon/polystyrene/air/silicon sandwich we find $Q \approx 6$. With an additional gold layer between the polymer film and the substrate Q is increased to ~ 83.[19]

Using Equation 2 the hydrodynamic response of the interface to the radiation pressure is calculated by a standard linear stability analysis.[11] The maximally amplified wavelength is given by

$$\lambda = 2\pi\left(-\frac{1}{2\gamma}\frac{\partial p}{\partial h}\right)^{-\frac{1}{2}} = 2\pi\sqrt{\frac{\gamma u \Delta T}{Q}\frac{\kappa_0\kappa_p}{(\kappa_p-\kappa_0)}\frac{1}{J_q}} \quad (3)$$

where γ is the polymer–air surface tension. The time for the film to become unstable is given by

$$\tau = \frac{3\eta}{\gamma h^3}\left(\frac{\lambda}{2\pi}\right)^4 \quad (4)$$

with the viscosity of the polymer melt η. Equation 3 predicts that the dominant wavelength in a setup with two flat silicon wafers (see Fig. 4) scales inversely with the heat flux. This is borne out by earlier studies.[18,19]

We now return to the setup in Figure 1. Due to the low thermal conductivity of air, the interfacial temperature—and therefore the strength of the interfacial pressure (Eq. 2)—depends on the width of the air gap ($d - h$). Since the thermal conductivity of silicon is much larger than that of the polymer and air, the topographic relief of the master pattern is an isothermal surface. The variation in the plate spacing d results in a lateral variation of the force field (radiation pressure). Such a laterally inhomogeneous field has two consequences. First, the instability is focused toward regions of highest fields, i.e., where ($d - h$) is smallest. The liquid polymer is drawn toward these protrusions. Second, τ is short at the lateral positions where the air-layer thickness $d - h$ is small (i.e., where the protrusions of the master extend down toward the polymer film). As predicted by Equation 4, $\tau \propto J_q^{-4} \propto (d-h)^4$, i.e., the time constant scales with the fourth power of the air gap. This implies a much earlier onset of the instability at lateral locations of the polymer film, which face the protrusions. Experimentally, this is illustrated by the blue region in the left part of Figure 2c, which corresponds to an unperturbed film at locations of a large air gap (corresponding to the left hand side of the schematic drawing in Fig. 1). At the same time, the instability has lead to a replication of the structured part of the master (right hand side of Fig. 2c). In this context, it is important to reemphasize that the instability depends on the applied temperature gradient. Samples annealed in an oven ($T_1 = T_2$) show neither the capillary instability of the polymer surface between planar plates, nor the pattern replication process.

We can use Equation 4 to estimate the time necessary for technological interesting length scales to evolve. For example, taking a periodicity of $\lambda = 50$ nm and an initial film thickness $h = \lambda/2$, $\tau \approx 0.4$ ms (for polystyrene at 170 °C: $\eta = 1.5 \times 10^4$ Ns m^{-2}, $\gamma = 3 \times 10^{-2}$ N m^{-1}). This time constant could be even further reduced by choosing a polymer with a lower viscosity.

The prediction and control of τ is important, however. Samples that have not been exposed to a temperature gradient for a sufficient period of time show no or only an incomplete replication of the topographic master. Leaving a sample for too long at film-destabilizing conditions is also detrimental. Such a sample not only shows pattern replication of the structured part of the master, but also instabilities reminiscent of Figure 4 at the locations of large air layer thicknesses $d - h$.

While the instability between two planar plates expresses a single length scale λ, this is not necessarily the case when a structured master is used. This is illustrated in Figure 2, where the hexagons of different sizes in (a–c) are all from the same sample, demonstrating that a range of length scales can be reproduced simultaneously under the same experimental conditions. Starting from a polystyrene film with $h = 65$ nm, 500 nm wide and 155 nm high lines were replicated in Figure 2d. The inset in (d) is a higher magnification atomic force microscopy (AFM) image, which allows us to quantitatively compare the replicated pattern with the template. The replicated radii of curvature of the intersecting lines are comparable to the template (see inset in Fig. 2d). The imperfect replication of the hexagons in (a), on the other hand, is due to a non-ideal choice of the ratio d/h. Since the hexagons occupy ≈ 50 % of the surface area, d/h should be ≈ 2. The value of $d/h = 1.5$ in (a) implies that more polymer than required has to be laterally accommodated. This, together with the polymer surface tension causes a rounding of the hexagons' corners. The result in (d), on the other hand, in which even small imperfections of the template are reproduced, shows that the replication process can be extended to lateral length scales of 100 nm or less.

Equation 3 allows one to predict whether this replication technique can be extended to smaller, technologically relevant lateral dimensions. While higher order terms in the surface energy may impose a cut-off at small length scales,[19] the replication of patterns down to 100 nm should in principle be possible, especially with a set-up in which Q is maximized.

 © 2003 WILEY-VCH Verlag GmbH & Co. KGaA, Weinheim 0935-9648/03/0603-0516 $ 17.50+.50/0

Taking for example $h = 25$ nm, $d = 50$ nm, $Q = 83$, and $\Delta T = 100$ K, we find for polystyrene and air (with $\kappa_0 = 0.034$ J $(\mathrm{m\,s\,K})^{-1}$ and $\kappa_p = 0.16$ J $(\mathrm{m\,s\,K})^{-1}$) $J_q \approx 100$ W mm^{-2}. Using these values, Equation 3 predicts $\lambda \approx 100$ nm.

Finally, we note the advantage of a positive replication technique over imprint lithography. The substantially reduced physical contact between the film and the master significantly decreases the effective adhesion between the master and the substrate. This facilitates the release of the master and reduces replication problems stemming from polymeric material that remains on the master after its release. The technique could be easily incorporated into existing fabrication lines and does not need any specialized equipment nor chemicals. Furthermore, a combination of such a thermomechanical instability with electrostatic forces[8] is a promising prospect for a simple, low-cost lithographic technique for the replication of sub-micrometer patterns.

Experimental

The polymer used was polystyrene (PS) with an averaged molecular weight of 108 kg mol^{-1} and a polydispersity of 1.03, purchased from Polymer Standards Service, Mainz and used as obtained. Highly polished silicon wafers were donated to us by Wacker Siltronic, Burghausen. Structured master wafers (by electron-beam lithography) were purchased from x'lith extreme lithography, Illerrieden. As received, all silicon wafers were covered with a native (≈ 2 nm thick) oxide layer. The silicon wafers were cleaned by a jet of carbon dioxide crystals ("snowjet" [22]). The structured master wafer was rendered apolar by deposition of a self-assembled alkane monolayer from solution [23] to minimize its adhesion to the polymer. Au was evaporated on the back side of all silicon wafers, improving the thermal contact and facilitating the short-circuiting of the two plates. Thin polymer films were prepared by spin-coating from analytic grade toluene onto the planar Si substrates. Typical polymer concentrations were 3 wt.-% and rotation speeds were ≈ 4000 rpm, resulting in film thicknesses h of around 100 nm. A topographically structured master wafer was mounted facing the polymer film, leaving an air gap. A schematic representation of the experimental set-up is shown in Figure 1. The plate spacing d was controlled by silicon dioxide spacers (dotted columns in Fig. 1), ranging from 100 to 600 nm. To eliminate the build up of electrostatic charges, both substrates were grounded. One side of the assembly was heated to a temperature T_1 by placing it onto a hot plate, while the other plate was cooled by bringing it into contact with a copper block set to a temperature T_2, which was temperature controlled by perfusion with water. Both temperatures were measured by small thermocouples (PT100) that were embedded into the copper blocks close to the Si wafers. Good thermal contact was ensured by thermal conducting paste. This established a temperature difference $\Delta T = T_1 - T_2$ of typically 10–50 K across the film–air double layer. Both temperatures were kept constant to within 1 K, above the glass transition temperature of the polymer to ensure the liquid state. Together with the small plate spacing this generates large temperature gradients on the order of 10^8 K m^{-1}. While pattern replication is typically completed after less than 1 h (see Eq. 4), we heated the samples over night to assure equilibration. Subsequently, the assembly was rapidly cooled to room temperature (below the glass transition temperature of the polymer). This quench freezes in the topographic structures of the polymer film, which can subsequently be conveniently analyzed or further processed at room temperature. The upper plate was mechanically removed, and the polymer films were characterized by optical and atomic force microscopy.

Received: September 4, 2002
Final version: November 12, 2002

[1] K. Ziemelis, *Nature* **2000**, *406*, 1021.
[2] R. Piner, J. Zhu, F. Xu, S. Hong, C. Mirkin, *Science* **1999**, *283*, 661.
[3] Y. Xia, J. A. Rogers, K. E. Paul, G. M. Whitesides, *Chem. Rev.* **1999**, *99*, 1823.
[4] S. Y. Chou, P. R. Krauss, *Science* **1996**, *272*, 85.
[5] S. Y. Chou, C. Keimel, J. Gu, *Nature* **2002**, *417*, 835.
[6] H. Schift, C. David, M. Gabriel, J. Gobrecht, L. Heyderman, W. Kaiser, S. Köppel, L. Scandella, *Microelectron. Eng.* **2000**, *53*, 171.
[7] M. Böltau, S. Walheim, J. Mlynek, G. Krausch, U. Steiner, *Nature* **1998**, *391*, 877.
[8] E. Schäffer, T. Thurn-Albrecht, T. P. Russell, U. Steiner, *Nature* **2000**, *403*, 874.
[9] Lord Rayleigh, *Proc. London Math. Soc.* **1878**, *10*, 4.
[10] A. Vrij, *Discuss. Faraday Soc.* **1966**, *42*, 23.
[11] F. Brochard-Wyart, J. Daillant, *Can. J. Phys.* **1990**, *68*, 1084.
[12] G. Reiter, *Phys. Rev. Lett.* **1992**, *68*, 75.
[13] R. Seemann, S. Herminghaus, K. Jacobs, *J. Phys.: Condens. Matter* **2001**, *13*, 4925.
[14] W. Mönch, S. Herminghaus, *Europhys. Lett.* **2001**, *52*, 525.
[15] S. Herminghaus, *Phys. Rev. Lett.* **1999**, *83*, 2359.
[16] S. Chou, L. Zhuang, L. Guo, *Appl. Phys. Lett.* **1999**, *75*, 1004.
[17] E. Schäffer, T. Thurn-Albrecht, T. P. Russell, U. Steiner, *Europhys. Lett.* **2001**, *53*, 518.
[18] E. Schäffer, S. Harkema, R. Blossey, U. Steiner, *Europhys. Lett.* **2002**, *60*, 255.
[19] E. Schäffer, S. Harkema, M. Roerdink, R. Blossey, U. Steiner, *Macromolecules* **2003**, *36*, 1645.
[20] E. Schäffer, U. Steiner, *Euro. Phys. J. E* **2002**, *8*, 347.
[21] R. Seemann, S. Herminghaus, K. Jacobs, *Phys. Rev. Lett.* **2001**, *86*, 5534.
[22] R. Sherman, D. Hirt, R. J. Vane, *J. Vac. Sci. Technol.* **1994**, *12*, 1876.
[23] P. Silberzan, L. Léger, D. Ausserré, J. J. Benattar, *Langmuir* **1991**, *7*, 1647.

Chemically Amplified Positive Resists for Two-Photon Three-Dimensional Microfabrication**

By *Tianyue Yu*, *Christopher K. Ober*,* *Stephen M. Kuebler*, *Wenhui Zhou*, *Seth R. Marder*,* and *Joseph W. Perry**

Two-photon excitation (TPE) provides a means for photoactivating chemical and physical processes with high spatial resolution in three dimensions, using a single tightly focused laser beam. TPE has enabled or furthered the development of several important new technologies, including three-dimensional (3D) fluorescence imaging,[1] 3D lithographic microfabrication (3DLM),[2–7] and new approaches to 3D optical data storage.[8,9] In each of these techniques, high spatial resolution is achievable because the two-photon absorption (TPA) probability depends quadratically on the excitation intensity. By tightly focusing an excitation beam, the region of two-photon absorption can be confined at the focus to a volume of the order of the cube of the excitation wavelength ($V \approx \lambda^3$). Any subsequent process, such as fluorescence or a photo-induced chemical reaction, is also localized to this small volume. Two-

[*] Dr. C. K. Ober, Dr. T. Yu
Materials Science and Engineering, Cornell University
Ithaca, NY 14853 (USA)
E-mail: cober@ccmr.cornell.edu
Prof. S. R. Marder, Dr. J. W. Perry, Dr. S. M. Kuebler, Dr. W. Zhou
Department of Chemistry, The University of Arizona
Tucson, AZ 85721 (USA)
E-mail: smarder@u-arizona.edu; jwperry@u-arizona.edu

[**] This research was supported by the National Science Foundation at Cornell University through the Nanobiotechnology Center (ECS-9876771) and at the University of Arizona through the Science and Technology Center for Materials and Devices for Information Technology Research (DMR-010967) and the Chemistry Division (CHE-0107105) and by the AFOSR through the Liquid Crystal MURI (#F49620-97-1-0014). Support from the W. M. Keck Foundation for the purchase of instrumentation used in this research is gratefully acknowledged. The Cornell Nanofabrication Facility is gratefully acknowledged for providing the equipment for initial photolithographic evaluation of the materials.

 © 2003 WILEY-VCH Verlag GmbH & Co. KGaA, Weinheim 0935-9648/03/0603-0517 $ 17.50+.50/0